ZEBRAFISH
Volume 10, Number 2, 2013

DOI: 10.1089/zeb.2013.0884

Multiple Ribosomal Proteins Are Expressed at High Levels in Developing Zebrafish Endoderm and Are Required for Normal Exocrine Pancreas Development

Elayne Provost,[1] Christopher A. Weier,[2] and Steven D. Leach[1–3]

Abstract

Ribosomal protein L (*rpl*) genes are essential for assembly of the 60S subunit of the eukaryotic ribosome and may also carry out additional extra-ribosomal functions. We have identified a common expression pattern for *rpl* genes in developing zebrafish larvae. After initially widespread expression in early embryos, the expression of multiple *rpl* genes becomes increasingly restricted to the endoderm. With respect to the pancreas, *rpl* genes are highly expressed in *ptf1a*-expressing pancreatic progenitors at 48 hpf, suggesting possible functional roles in pancreatic morphogenesis and/or differentiation. Utilizing two available mutant lines, *rpl23a*^{hi2582} and *rpl6*^{hi3655b}, we found that *ptf1a*-expressing pancreatic progenitors fail to properly expand in embryos homozygous for either of these genes. In addition to these durable homozygous phenotypes, we also demonstrated recoverable delays in *ptf1a*-expressing pancreatic progenitor expansion in *rpl23a*^{hi2582} and *rpl6*^{hi3655b} heterozygotes. Disruptions in ribosome assembly are generally understood to initiate a p53-dependent cellular stress response. However, concomitant p53 knockdown was unable to rescue normal pancreatic progenitor expansion in either *rpl23a*^{hi2582} or *rpl6*^{hi3655b} mutant embryos, suggesting required and p53-independent roles for *rpl23a* and *rpl6* in pancreas development.

Introduction

Ribosome assembly is a complex mechanism requiring 79 ribosomal proteins (RPs) and over 150 nonribosomal proteins.[1] Proper ribosome biogenesis maintains normal protein translation and is an essential cellular function. As such, proteins required for ribosome assembly are robustly and ubiquitously expressed. During times of rapid proliferation, such as during development, the demand for functional ribosomes becomes even greater.[2]

RPs are involved in assembly of either the small 40S or the large 60S ribosomal subunits and, as such, are designated Rps or Rpl. Similar to the mouse and human genomes, there are 30 *rps* genes and 40 *rpl* genes annotated in the zebrafish genome. A previous study using morpholino knockdown of a large cohort of these *rps* and *rpl* genes in developing zebrafish suggested that a variety of axis defects and abnormalities in the CNS could be uniquely assigned to individual RPs. These data and additional studies point to the possibility of previously unappreciated tissue-specific requirements for individual RPs.[3]

In addition to morpholino studies, an advantage of the zebrafish among vertebrate model organisms is its large collection of genetic mutants in RP genes. An early retroviral screen identified and phenotypically characterized 28 mutant RP lines.[4] As homozygotes, these lines exhibited many gross developmental defects and generally resulted in embryonic lethality. Among the zebrafish RP mutants identified, defects in the endoderm-derived tissues were frequently noted in homozygous embryos. However, because the development of endoderm-derived tissues occurs relatively late in embryonic life, it is unclear whether endodermal abnormalities observed in RP mutants are caused by pleiotrophic effects, or represent cell-autonomous roles in endodermal organogenesis.

Recently, we identified an essential role for three genes related to ribosome biogenesis in early pancreas development. Using both mutants and morpholino knockdown of the *rpl3,* pescadillo (*pes*), and Shwachman–Bodian–Diamond syndrome (*sbds*) genes, we demonstrated that loss of any of these genes early in development resulted in altered pancreatic morphogenesis, with preserved endocrine and exocrine differentiation.[5] Mutations in genes related to ribosome

[1]Department of Surgery, [2]Graduate Training Program in Cellular and Molecular Medicine, and [3]McKusick-Nathans Institute of Genetic Medicine, Johns Hopkins University, Baltimore, Maryland.

biogenesis are generally understood to cause a p53-mediated cellular stress response, and a concomitant loss of p53 is often able to rescue loss-of-function phenotypes (reviewed[6]). However, we discovered that, with respect to the expansion of pancreatic progenitors in developing zebrafish, loss of p53 did not rescue *rpl3, pes,* or *sbds* mutant embryos.[5]

To extend our initial studies suggesting an essential role for genes related to ribosome biogenesis in pancreatic progenitor expansion, we evaluated expression of a large cohort of *rpl* genes in developing zebrafish. One hypothesis would be that the genes that play an instructive role in endoderm development would be expressed in early endodermal precursors and represent a tissue-specific cohort of RPs responsible for pancreatic progenitor expansion. To determine whether we could detect tissue-specific expression patterns for *rpl* genes, we performed *in situ* hybridization for the majority of the identified *rpl* genes. We found that these genes displayed a shared expression pattern, typically characterized by initially ubiquitous expression at 24 hpf, but with high-level expression restricted to liver and pancreas by 5 dpf. Interestingly, all examined *rpl* genes displayed strong expression in embryonic pancreatic progenitor cells at 48 hpf. On the basis of this expression pattern, we performed a detailed characterization of pancreatic development in two zebrafish mutants, *rpl23a*^{hi2582} and *rpl6*^{hi3655b}, to determine whether these genes were required for normal pancreatic progenitor function. We found that both *rpl23a*^{hi2582} and *rpl6*^{hi3655b} failed to expand their normal pool of pancreatic progenitors not only in homozygous mutant embryos, but in heterozygotes as well. Finally, we tested whether these mutants could be rescued by concomitant knockdown of p53 and discovered that the *rpl23a*-^{hi2582} and *rpl6*^{hi3655b} pancreatic phenotype is p53 independent. We conclude that similar to our previously reported results for *rpl3, pes,* and *sbds*, loss of either *rpl23a*^{hi2582} or *rpl6*^{hi3655b} results in a failure of early pancreatic morphogenesis, independent of p53 expression. Together, these data suggest previously unappreciated and essential roles for multiple *rpl* genes in vertebrate pancreas development.

Materials and Methods

Fish strains, genotyping, morpholinos, and embryo injections

All fish were raised using standard husbandry procedures. The following fish strains were used in this study: Tg BAC ptf1a:eGFP^{jh1},[7] Tg Tol2 ins:mCherry^{jh2},[8] rpL23a^{hi2582} (obtained from Zirc, Eugene, OR), and rpL6^{hi3655b} (obtained from Zirc). Tail fins of adult fish, or individual larvae were digested in low TE (10 mM Tris HCl 7.5, 1 mM EDTA) plus proteinase K at 55°C. PCR genotyping was done to confirm the retroviral insertion in the *rpL23a*^{hi2582} locus (forward primer 5′ CGAAG GCGAAGAAGGAAGGTG, reverse primer 5′ GTTCCTTG GGAGGGTCTCCTC) and wild-type *rpl23a* locus (forward primer, 5′ CAGGCAATTGACACTTTGTTAG, reverse primer 5′ CAATTGTACGTGAACATGAAGG). PCR genotyping was done to confirm the retroviral insertion in the *rpL6*^{hi3655b} locus (forward primer 5′ GAATGGCTTTGGTCAAATTGCTG, reverse primer 5′ GCTAGCTTGCCAAACCTACAGGT). The standard p53^{ATG} morpholino (MO) was obtained from Gene Tools (Philomath, OR), resuspended in water, and injected at 1 ng into 1–4-cell zebrafish embryos. Embryos were subsequently raised at 28°C in embryo water plus PTU to inhibit pigmentation.

Microscopy

Live embryos were anesthetized with Tricaine, embedded in agarose (low melt agarose 1.5%, sucrose 1%, in embryo water), and immobilized on coverslips. Confocal imaging was done using UV, argon, and He/Ne lasers for blue, green, and red channels, respectively, using a Nikon A1Rsi system.

In situ *hybridization*

Whole-mount *in situ* hybridization was conducted as previously described.[9] To perform *in situ* hybridization on paraffin sections, 12 μm sections were deparaffinized in histoclear and rehydrated. Sections were prehybridized (50% formamide, 5× SSC pH 4.5 w/citric acid, 50 μg/mL yeast tRNA, 1% SDS, 50 μg/mL heparin) at 55°C for 2 h. Anti-sense *in situ* probes were boiled in prehybridization buffer (10 μL/mL), added to tissue sections, covered with a coverslip and hybridized at 68°C in a humidity chamber overnight. Tissue sections were washed in 5× SSC at 68°C, followed by 0.2× SSC at 68°C and Maelic acid buffer (MAB) at room temperature. Sections were blocked in 10% sheep serum diluted in MAB for 1 h and incubated with anti-digoxigenin alkaline phosphatase antibody at 1:5000 overnight at 4°C. Slides were washed with MAB + 0.1% Tween-20, and signal was detected using BM purple at room temperature. Reactions were stopped with 1 mM EDTA pH 8.0, dehydrated, mounted, and imaged. Antisense digoxigenin-labeled RNA probes were amplified for trypsin,[9] insulin,[10] *rpL4* (forward primer 5′ CTC GGT CTA CTC CGA GAA AG, reverse primer 5′ CCA TGC CTT TAG CTT CTT CAA C), *rpL6* (forward primer 5′ ATG GCT GAG GGC GAT AAG, reverse primer 5′ TTA GAA AAC CAG TTT GTG TGG G), *rpL8* (forward primer 5′ ATG GGA CGT GTG ATC AGG, reverse primer 5′ CTC GCA GTC TGC CAG TAC), *rpL9* (forward primer 5′ ATG AAG ACC ATT CTC AGT AAC CAG, reverse primer 5′ TTA GTC CTC TTG CTG TTC CAC), *rpL11* (forward primer 5′ ATG AGG GAG CTG CGC ATC, reverse primer 5′ GGG AGG ATG ATG CCG TCA TAC), *rpL12* (forward primer 5′ ATG CCT CCT AAA TTC GAC CC, reverse primer 5′ CTC AGT TGG GCA CTC AAC), *rpL15* (forward primer 5′ ATG GGA GCG TAC AAG TAT ATG C, reverse primer 5′ CTA GCG GTA ACG GTG CAG), *rpL18a* (forward primer 5′ ATG AAG GCG TCT GGC ACA C, reverse primer 5′ TGG TCT CTT GGT GGT GAA GC), *rpL19* (forward primer 5′ GAA GAG GCT GGC CTC CAG, reverse primer 5′ CCT CGC GAC GCT TAC GAG), *rpL21* (forward primer 5′ ATG ACT AAC ACC AGA GGC AAG, reverse primer 5′ GCC ATA AAC TCG TAT GGG ATG G), *rpL23* (forward primer 5′ ATG TCT AAG AGA GGA CGT GGT GG, reverse primer 5′ TCA GGC AAT GCT GCC AGC), *rpL23a* (forward primer 5′ ATG GCC CCG AAG GCG AAG, reverse primer 5′ TTA GAT GAT GCC GAT CTT GTT GGC AAC), *rpL24* (forward primer 5′ ATG AAG GTC GAG CTG TGC, reverse primer 5′ TTA GCG TTT GCC ACC GAC), *rpL27* (forward primer 5′ GAA ACC TGG CAA GGT GGT G, reverse primer 5′ CGG AGC TTC TGG AAG AAC C), *rpL28l* (forward primer 5′ ATG GCA TCG CCT CAC CTG, reverse primer 5′ CTT GGG AGC CCT GGA GC), *rpL30* (forward primer 5′ ATG GTG GCC GCA AAG AAG, reverse primer 5′ CTG GTC TGG CAT ACT CCT GAT G), *rpL34* (forward primer 5′ ATG GTG CAG CGC CTG AC, reverse primer 5′ CTT CGA CTT CTG GGT CTG TGC C), *rpL35a* (forward primer 5′ GGC TAC AAG CGT GGC CTG, reverse primer 5′ CGA ATT

CTG TGC CCG ATA GCC), *rpL36* (forward primer 5′ ATG GTT GTC AGA TAT CCT ATG GC, reverse primer 5′ CTA CTC TTT CTT GGC AGC AG), *rpL36a* (forward primer 5′ ATG GTA AAC GTT CCG AAG ACC, reverse primer 5′ TTA AAA CTG GAT GAC CTG GCC), and *rpL37* (forward primer 5′ ATG ACG AAG GGT ACG TCG, reverse primer 5′ TTA TGA GGA GCT GGA CGC). All probes were validated by confirming negligible labeling by sense controls.

Results

Multiple rpl *genes are expressed in similar patterns during zebrafish development*

We undertook a broad survey of *rpl* gene expression patterns in developing zebrafish embryos. *In situ* probes were generated from zebrafish embryonic total cDNA and sequence verified. Sense and anti-probes were tested in the developmental series of wild-type AB embryos at 24, 48, 72, and 120 hpf and assessed for their tissue-specific staining patterns. Because we identified endodermal expression with all of the probes we tested, a cohort of *in situ* probes was also used in two-color *in situ*s with a fluorescein-labeled insulin probe to identify the primary islet. For each examined *rpl* gene, a similar expression pattern was observed, as exemplified by *rpl36a* (Fig. 1A). At 24 hpf, expression of *rpl36a* is broad in all tissues. By 48 hpf, expression is strongest in the CNS, pharyngeal arches, and endoderm, which is best visualized after yolk removal. At 48 hpf, expression of *rpl36a* is clearly evident in pancreatic progenitors surrounding the primary islet. At this stage, the principal islet expresses both insulin and *rpl36a*, resulting in a signal that appears darker than in other adjacent endodermal tissues. *Rpl36a* is also expressed in the developing liver and intestine (Fig. 1A and data not shown). Expression in endoderm-derived tissues continues throughout development and at 5 dpf remains particularly strong in the mature, differentiated cells of exocrine pancreas (Fig. 1A).

In addition to examining the expression of multiple *rpl* genes during development, we also evaluated their expression in adult zebrafish endoderm, using *in situ* hybridization on paraffin sections. Similar to their developmental expression patterns, all examined *rpl* genes displayed similar high-level epithelial expression in the liver, pancreas, and intestine, again as exemplified by *rpl36a* (Fig. 1B). In sections that also included tissue from the spleen, there was no expression detected above sense controls for any of the *rpl* genes.

In other vertebrates, adult liver and pancreas are known to have high levels of *rpl* expression. Polysome isolation to evaluate ribosome subunit ratios is routinely performed from mouse or rat liver,[11] and adult acinar cells are characterized by an extremely dense elaboration of rough endoplasmic reticulum. Because of the high demands for protein translation displayed by acinar cells, it was not surprising to us to observe high-level expression of *rpl* genes in adult pancreas. More surprising was the high-level expression of multiple *rpl* genes observed in pancreatic cells at 48 hpf, before the onset of cellular differentiation and digestive enzyme expression (Fig. 1). For all examined *rpl* genes, high-level expression was observed in developing pancreas, as well as in developing liver and intestine (Fig. 1C). On the basis of these expression patterns as well as our earlier observation that loss of *rpl3* resulted in defective proliferation of pancreatic progenitor cells,[5] we next evaluated two *rpl* genetic mutants, *rpl23a*^{hi2582}

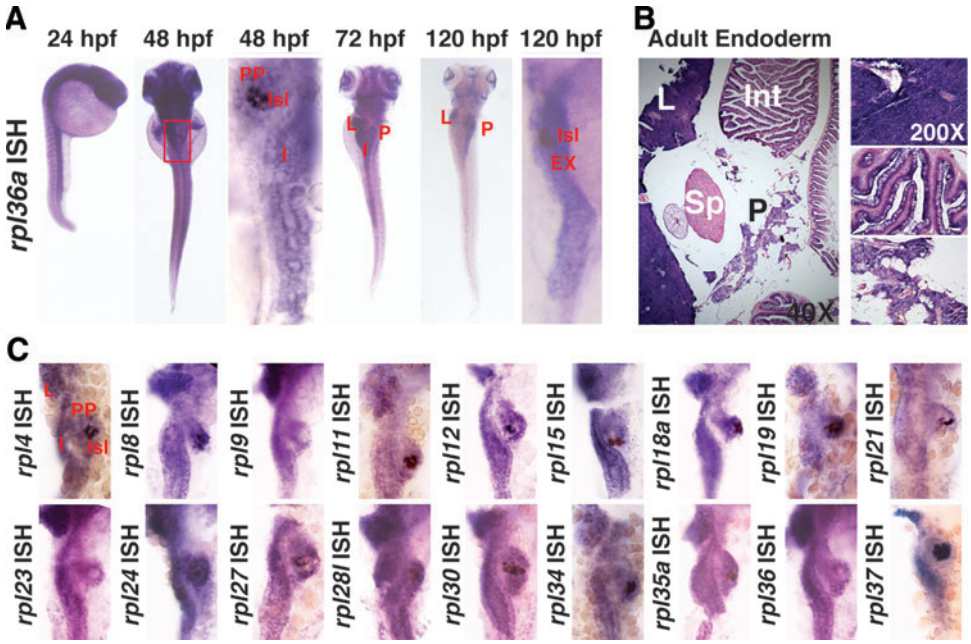

FIG. 1. Ribosomal protein l (*rpl*) genes are broadly expressed in wild-type zebrafish endoderm. **(A)** Expression of *rpl36a* during zebrafish development. At 24 hpf, expression is broad in all tissues. During the course of development, expression becomes increasingly restricted to the larval endoderm. rpL9, 23, and 36 represent single color *in situ*s; the remaining panels depict two-color *in situ* hybridization for the indicated *rpL* gene in *blue* and insulin in *red*. **(B)** *rpl36a* is strongly expressed in epithelial cells of the adult liver, intestine, and pancreas. **(C)** At 48 hpf, many *rpL* genes are expressed in a similar pattern in endodermal progenitors. L, liver; I, intestine; P, pancreas; Ex, exocrine pancreas; Isl, islet of Langerhans; PP, pancreatic progenitors; Sp, spleen. Color images available online at www.liebertpub.com/zeb

and *rpl6*^{hi3655b}, to determine whether loss-of-function mutations in multiple *rpl* genes might converge upon a common phenotype.

Rpl23a *is expressed in exocrine pancreatic progenitor cells and is required for normal pancreas development*

Similar to the expression pattern of other *rpl* genes, *rpl23a* exhibits broad expression in all tissues at 24 hpf, followed by increasing restriction to endoderm-derived tissues later in development. High-level expression was observed in the developing liver, intestine, and pancreas at 48 hpf (Figs. 1C and 2A), with similar high-level epithelial expression observed in these tissues in adults (Fig. 2B).

We obtained a mutant for *rpl23a*^{hi2582} and crossed it to our double transgenic reporter line, *ptf1a:eGFP*^{jh1}*;ins:mCherry*^{jh2}. This combination of transgenic alleles labels undifferentiated progenitor cells and differentiated adult acinar cells in green, and developing and adult β-cells in red, allowing direct examination of pancreatic phenotypes in live embryos. Previous descriptions of *rpl23a*^{hi2582} mutant embryos suggested an underdeveloped liver/pancreas late in development, at 5 dpf, as appreciated by gross inspection of embryos (web.mit.edu/hopkins/group11.html). An incross of *rpl23a*$^{hi2582/+}$; *ptf1a:eGFP*^{jh1}*;ins:mCherry*^{jh2} adults resulted in 29% of the resulting clutch exhibiting abnormal morphology at 72 hpf, consistent with the recessive nature of this mutation. This mutant phenotype included delayed pigmentation, reduction in the size of the head and eye, mild edema, and poor yolk absorption (Fig. 2C, D). Embryos produced from an *rpl23a*$^{hi2582/+}$*;ptf1a:eGFP*^{jh1}*;ins:mCherry*^{jh2} outcross were used as controls, and exhibited only a 1.6% incidence of abnormal

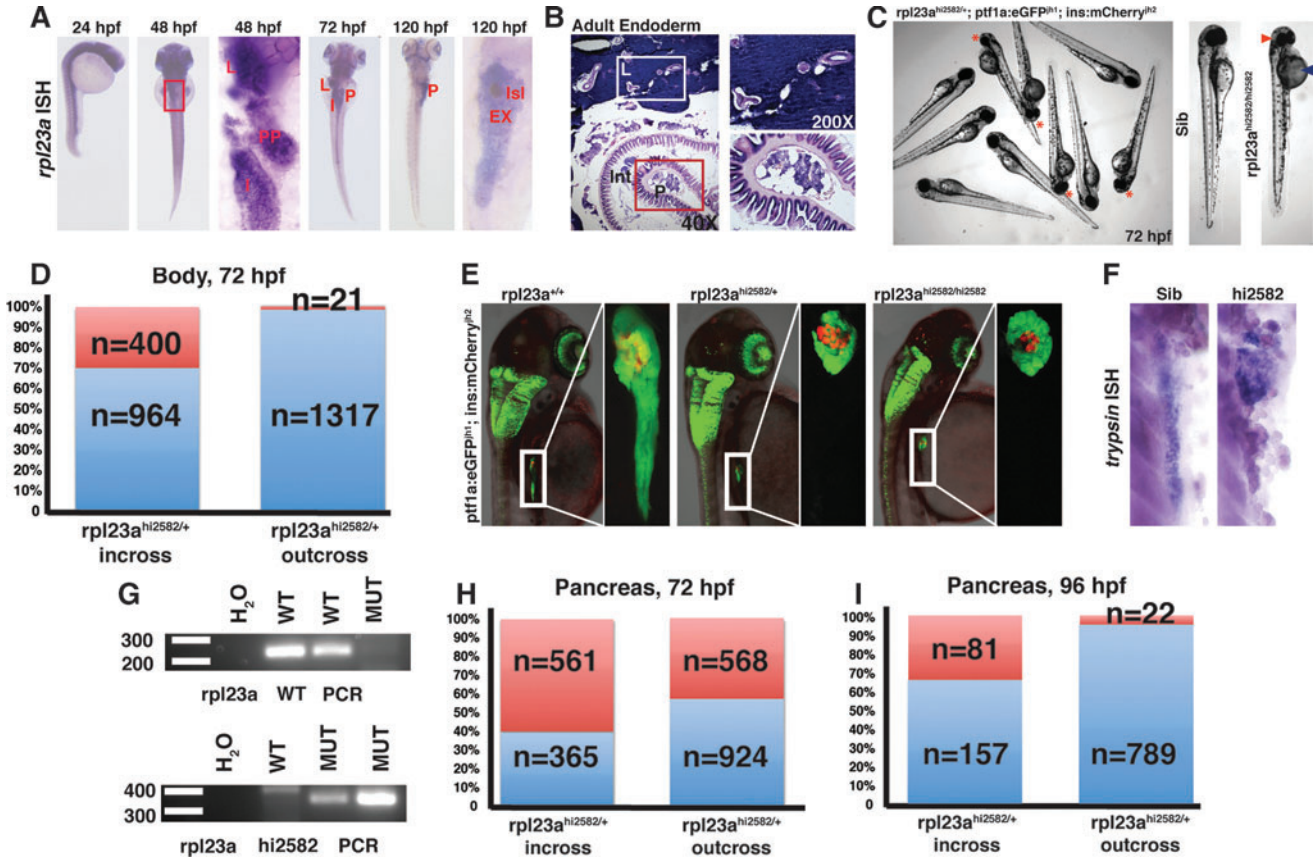

FIG. 2. Mutations in the *rpl23a* gene result in compromised expansion of *ptf1a*-expressing pancreatic progenitor cells. **(A)** Expression of *rpl23a* during zebrafish development is broad at 24 hpf and becomes increasingly restricted to the larval endoderm during the course of development. **(B)** Strong expression of *rpL23a* is observed in adult liver, intestine, and pancreas. **(C)** An incross of *rpl23a*$^{hi2582/+}$*;ptf1a:eGFP*^{jh1}*;ins:mCherry*^{jh2} adult fish results in 72 hpf embryos exhibiting reduced brain and eye size (*red arrowhead*), edema, and poor yolk absorption (*blue arrowhead*). **(D)** Fraction of embryos from *rpl23a*$^{hi2582/+}$*;ptf1a:eGFP*^{jh1}*;ins:mCherry*^{jh2} incross displaying gross developmental defects as assessed at 72 hpf (29% mutant, *red*; 71%, wild type, *blue*) compared with control embryos generated by *rpl23a*$^{hi2582/+}$*;ptf1a:eGFP*^{jh1}*;ins:mCherry*^{jh2} outcross (2.8% mutant, *red*; 97.2% wild type, *blue*). **(E)** *ptf1a*-expressing pancreatic progenitor cells fail to expand normally in embryos generated by *rpl23a*$^{hi2582/+}$*;ptf1a:eGFP*^{jh1}*;ins:mCherry*^{jh2} incross. **(F)** Activation of trypsin expression occurs normally in *rpl23a*$^{hi2582/hi2582}$ hypoplastic pancreas. Images in (E) and (F) obtained at 72 hpf. **(G)** PCR genotyping of embryos individually imaged at 72 hpf confirms reduced pancreatic mass in both heterozygous *rpl23a*$^{hi2582/+}$*;ptf1a:eGFP*^{jh1}*; ins:mCherry*^{jh2} and homozygous *rpk23a*$^{hi2582/hi2582}$*;ptf1a:eGFP*^{jh1}*; ins:mCherry*^{jh2} embryos. **(H)** Incidence of abnormal pancreas development in embryos produced by either incross or outcross *rpl23a*$^{hi2582/+}$*;ptf1a:eGFP*^{jh1}*; ins:mCherry*^{jh2} adults, expressed as the fraction of phenotypic (*red*) and wild-type (*blue*) embryos evaluated at 72 hpf. **(I)** Decreased incidence of persistent hypoplastic pancreas at 96 hpf indicates recovery of normal pancreatic mass in *rpl23a*$^{hi2582/+}$ heterozygotes. Color images available online at www.liebertpub.com/zeb

gross morphology, demonstrating that *rpl23a*$^{hi2582/+}$ heterozygotes undergo grossly normal development.

Next we examined pancreatic development in 72 hpf embryos produced by incrossing *rpl23a*$^{hi2582/+}$;*ptf1a:eGFP*^{jh1};*ins:mCherry*^{jh2} fish. In contrast to the gross morphological defects observed in ~25% of resulting embryos (Fig. 2C, D), we identified defective expansion of *ptf1a*-expressing pancreatic progenitors in 61% of the embryos (Fig. 2E, H). Moreover, a similar initial defect in pancreatic development was observed in 37.5% of embryos resulting from an *rpl23a*$^{hi2582/+}$;*ptf1a:eGFP*^{jh1};*ins:mCherry*^{jh2} outcross. Together, these findings suggested both fully penetrant homozygous and at least partially penetrant haploinsufficient phenotypes. In both scenarios, the observed decrease in pancreatic volume was associated with maintained expression of trypsin, suggesting a specific morphogenetic defect with maintenance of normal differentiation (Fig. 2F).

To confirm both homozygous and haploinsufficient phenotypes, we imaged individual embryos resulting from an *rpl23a*$^{hi2582/+}$;*ptf1a:eGFP*^{jh1};*ins:mCherry*^{jh2} incross, followed by PCR genotyping. This analysis confirmed that *rpl23a*$^{hi2582/+}$ heterozygotes displayed consistently reduced pancreatic volumes at 72 hpf (Fig. 2E, G). Because *rpl23a*$^{hi2582/+}$;*ptf1a:eGFP*^{jh1};*ins:mCherry*^{jh2} embryos can be successfully raised to adulthood, we wondered whether pancreatic progenitor expansion in *rpl23a*$^{hi2582/+}$ heterozygote embryos at 72 hpf was merely delayed, and would subsequently recover to generate a normal pancreatic mass. To answer this question, we also examined embryos generated by an *rpl23a*$^{hi2582/+}$;*ptf1a:eGFP*^{jh1};*ins:mCherry*^{jh2} incross at 96 hpf, and found that the fraction of embryos with defective pancreatic morphogenesis was reduced to 34%. Additionally, by 96 hpf the fraction of embryos displaying abnormal pancreas development within clutches generated by an *rpl23a*$^{hi2582/+}$;*ptf1a:eGFP*^{jh1};*ins:mCherry*^{jh2} outcross was reduced to 2.7% (Fig. 2I). To rule out the possibility that this apparent recovery of pancreas mass might be caused by selective death of phenotypic embryos between 72 and 96 hpf, we quantified survival between these two time points, and observed the survival rates to be 97% for the incross and 95% for the outcross (data not shown). Therefore, recovery of the pancreas phenotype is not caused by selective death of embryos with defective pancreatic morphogenesis.

These data demonstrate that *rpl23a*$^{hi2582/hi2582}$;*ptf1a:eGFP*^{jh1};*ins:mCherry*^{jh2} homozygous embryos exhibit multiple phenotypes, including a reduction in brain and eye size, edema, and poor yolk absorption, as well as a failure of *ptf1a*-expressing pancreatic progenitor cells to properly expand. Additionally, *rpl23a*$^{hi2582/+}$;*ptf1a:eGFP*^{jh1};*ins:mCherry*^{jh2} heterozygotes, while appearing grossly normal, exhibit a recoverable delay in pancreas development.

Rpl6 *is expressed in exocrine pancreatic progenitor cells and is required for normal pancreas development*

On the basis of the observed defect in pancreas development in *rpl23a*^{hi2582} mutant embryos, we were curious whether a failure of pancreatic progenitor expansion represented a common phenotype among other *rpl* mutants. We therefore performed a similar analysis using a second *rpl* mutant, *rpl6*^{hi3655b}. As with all the other *rpl* genes tested, *rpl6* demonstrates ubiquitous expression at 24 hpf, followed by increasing restriction to endoderm-derived tissues over the course of development. Again, at 48 hpf, expression was high in developing liver, intestine, and pancreas (Fig. 3A), and remained high in these tissues in the adult (Fig. 3B).

We obtained a mutant *rpl6*^{hi3655b} line, which in our hands was a more subtle mutant than *rpl23a*^{hi2582}, previously described as having an underdeveloped liver and gut at 5 dpf (web.mit.edu/hopkins/group10.html). The *rpl6*^{hi3655b} allele was crossed onto a *ptf1a:eGFP*^{jh1};*ins:mCherry*^{jh2} background, allowing us to evaluate the role of *rpl6* in pancreas development. Among embryos generated by an *rpl6*$^{hi3655b/+}$;*ptf1a:eGFP*^{jh1};*ins:mCherry*^{jh2} incross, gross morphologic abnormalities were evident by 96 hpf, including a small head, underdeveloped brain, edema, and poor yolk absorption (Fig. 3C). Grossly phenotypic embryos from the *rpl6*$^{hi3655b/+}$;*ptf1a:eGFP*^{jh1};*ins:mCherry*^{jh2} incross represented 20.2% of the total clutch, as expected for a recessive trait. In contrast, only 1.7% of embryos produced by an *rpl6*$^{hi3655b/+}$;*ptf1a:eGFP*^{jh1};*ins:mCherry*^{jh2} outcross displayed gross phenotypic abnormalities (Fig. 3D).

The adult pancreas is normal in *rpl6*$^{hi3655b/+}$;*ptf1a:eGFP*^{jh1};*ins:mCherry*^{jh2} heterozygotes. When the abdominal viscera from healthy adult heterozygotes are examined, the pancreas appears normal in both size and structure. This includes the presence of both the primary and secondary islets (Fig. 3E; mCherry, yellow and white arrows) a normal exocrine pancreatic volume (Fig. 3E; eGFP), and entirely normal pancreatic histology (Fig. 3E).

To determine whether rpl6 was required for normal pancreas development, we individually imaged 72 hpf embryos generated by both incrosses and outcrosses of *rpl6*$^{hi3655b/+}$;*ptf1a:eGFP*^{jh1};*ins:mCherry*^{jh2} fish. This revealed defective expansion of *ptf1a*-expressing pancreatic progenitors in 43.2% of embryos produced by the *rpl6*$^{hi3655b/+}$;*ptf1a:eGFP*^{jh1};*ins:mCherry*^{jh2} incross (Fig. 3F, H), and 30.7% of embryos produced by the *rpl6*$^{hi3655b/+}$;*ptf1a:eGFP*^{jh1};*ins:mCherry*^{jh2} outcross. In all embryos examined, the small pancreas phenotype was associated with normal expression of *trypsin*, again suggesting a selective defect in progenitor numbers but not in progenitor differentiation (Fig. 3G).

While the fraction of embryos with an undersized pancreas was not as striking in the *rpl6*$^{hi3655b/+}$;*ptf1a:eGFP*^{jh1};*ins:mCherry*^{jh2} incross as the *rpl23a*$^{hi2582/+}$;*ptf1a:eGFP*^{jh1};*ins:mCherry*^{jh2} incross, it was still elevated above the 25% expected for a purely recessive trait. Therefore, we again suspected that some fraction of heterozygous *rpl6*$^{hi3655b/+}$;*ptf1a:eGFP*^{jh1};*ins:mCherry*^{jh2} embryos was also displaying the hypoplastic pancreatic phenotype, and that these heterozygotes might demonstrate phenotypic recovery, similar to *rpl23a*$^{hi2582/+}$;*ptf1a:eGFP*^{jh1};*ins:mCherry*^{jh2} heterozygotes. Indeed, when embryos from an *rpl6*$^{hi3655b/+}$;*ptf1a:eGFP*^{jh1};*ins:mCherry*^{jh2} incross clutches were examined at 96 hpf, only 26.7% of the clutch exhibited a reduction in the pancreas size. Similarly, the fraction of embryos from *rpl6*$^{hi3655b/+}$;*ptf1a:eGFP*^{jh1};*ins:mCherry*^{jh2} outcross displaying an abnormal pancreas was reduced to 10% at 96 hpf. Thus, similar to *rpl23a*^{hi2582}, *rpl6*^{hi3655b} haploinsufficient embryos display a recoverable delay in pancreas development, with an initially hypoplastic pancreas at 72 hpf undergoing complete recovery over the next 24 h. Again we confirmed that this improvement was not caused by selective death of phenotypic embryos, as survival between 72 and 96 hpf was 93% for embryos generated by the incross, and 96% for embryos generated by the outcross (data not shown).

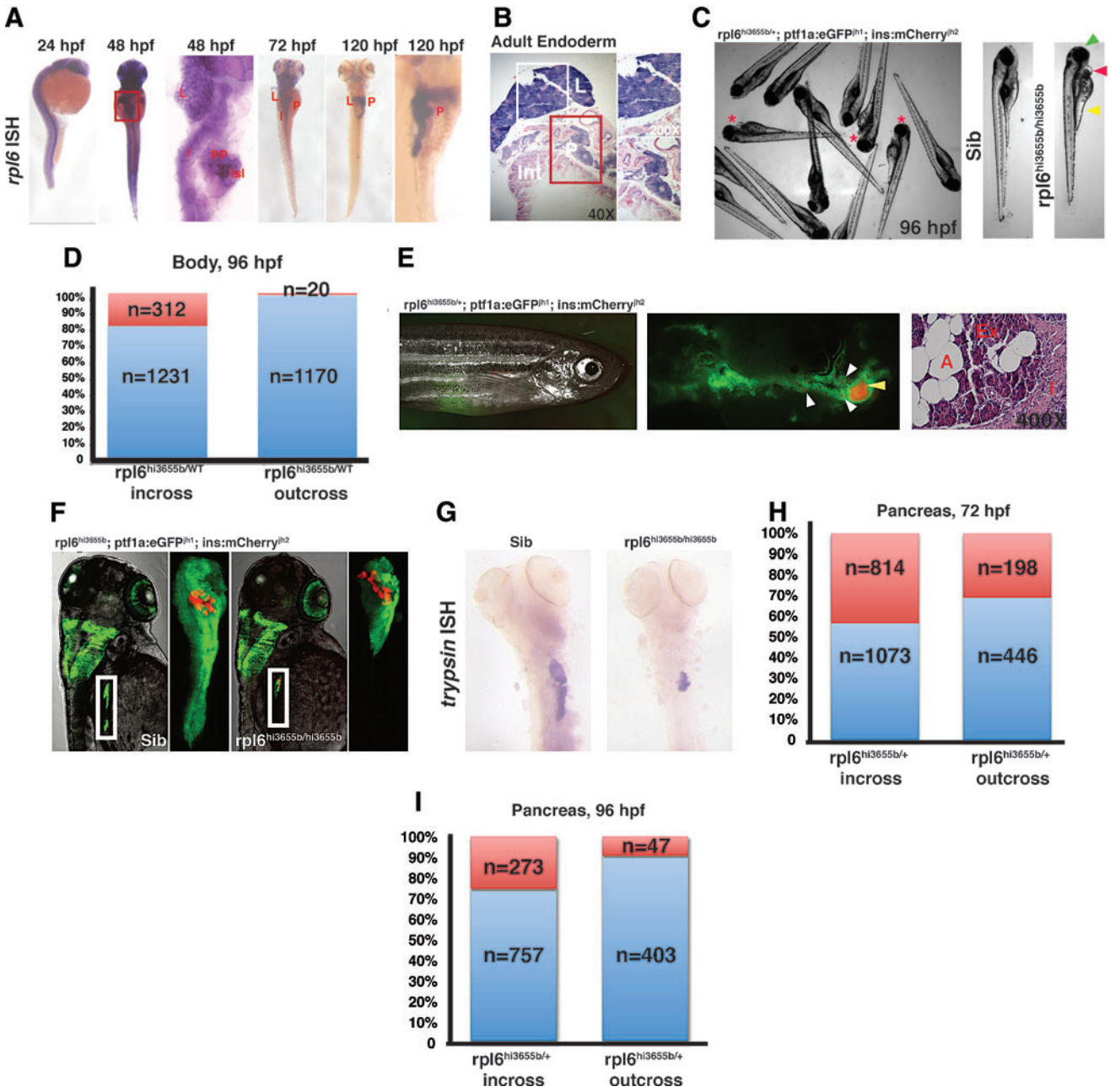

FIG. 3. Mutations in the *rpl6* gene result in compromised expansion of *ptf1a*-expressing pancreatic progenitor cells. **(A)** *rpl6* expression is initially broad at 24 hpf, but high-level expression becomes increasingly restricted to the larval endoderm during the course of development. **(B)** Strong expression of *rpl6* is observed in adult liver and pancreas. **(C)** An incross of *rpl6*$^{hi3655b/+}$;*ptf1a:eGFP*^{jh1};*ins:mCherry*^{jh2} adult fish results in 72 hpf embryos exhibiting reduced brain and eye size (*green arrowhead*), edema (*red arrowhead*), and poor yolk absorption (*yellow arrowhead*). Asterisks indicate grossly phenotypic *rpl6*$^{hi3655b/hi3655b}$ embryos. **(D)** Fraction of embryos from *rpl6*$^{hi3655b/+}$;*ptf1a:eGFP*^{jh1};*ins:mCherry*^{jh2} incross displaying gross developmental defects as assessed at 72 hpf (21% mutant, *red*; 79% wild type, *blue*) compared with control embryos generated by *rpl6*$^{hi3655b/+}$;*ptf1a:eGFP*^{jh1};*ins:mCherry*^{jh2} outcross (1.7% mutant, *red*; 98.3% wild type, *blue*). **(E)** The adult pancreas is grossly and histologically normal in *rpl6*$^{hi3655b/+}$;*ptf1a:eGFP*^{jh1};*ins:mCherry*^{jh2} heterozygotes. Note normal gross appearance of 7-month-old heterozygote, grossly normal pancreas including acinar cell mass (*green*), principal islet (*yellow arrowhead*), and secondary islets (*white arrowheads*), as well as normal adult histology. **(F)** *ptf1a*-expressing pancreatic progenitor cells fail to expand normally in embryos generated by *rpl6*$^{hi3655b/+}$;*ptf1a:eGFP*^{jh1};*ins:mCherry*^{jh2} incross. **(G)** Activation of trypsin expression occurs normally in *rpl6*$^{hi3655b/hi3655b}$ hypoplastic pancreas. **(H)** Incidence of abnormal pancreas development in embryos produced by either incross or outcross *rpl6*$^{hi3655b/+}$;*ptf1a:eGFP*^{jh1}; *ins:mCherry*^{jh2} adults, expressed as the fraction of phenotypic (*red*) and wild-type (*blue*) embryos evaluated at 72 hpf. **(I)** Decreased incidence of persistent hypoplastic pancreas at 96 hpf indicates recovery of normal pancreatic mass in *rpl6*$^{hi3655b/+}$ heterozygotes. A, adipose tissue. Color images available online at www.liebertpub.com/zeb

On the basis of these results, we conclude that *rpl6*$^{hi3655b/hi3655b}$;*ptf1a:eGFP*^{jh1}; *ins:mCherry*^{jh2} homozygous embryos exhibit a variety of developmental defects, including altered brain development and a failure of pancreatic progenitors to properly expand. Additionally, *rpl6*$^{hi3655b/+}$;*ptf1a:eGFP*^{jh1}; *ins:mCherry*^{jh2} heterozygotes, while appearing grossly normal, exhibit a recoverable delay in pancreas development. Thus, we conclude that multiple *rpl* genes are required for normal expansion of *ptf1a*-expressing pancreatic progenitor cells in the developing zebrafish embryo.

Loss of p53 does not rescue expansion of ptf1a-*expressing pancreatic progenitor cells in* rpl23a^{hi2582} *or* rpl6^{hi3655b} *mutant embryos*

Previous work with a variety of RP mutants has suggested a p53-dependent mechanism mediating the phenotypes associated with RP disruption. Several animal models of human diseases caused by mutations in RPs, such as Treacher–Collins disease, 5q − syndrome, and Diamond–Blackfan anemia, have all demonstrated that concomitant knockdown of p53 ameliorates the disease phenotype associated with ribosome dysfunction in various model organisms.[12–18] However, we previously demonstrated that loss of p53 is unable to rescue multiple phenotypes associated with a zebrafish model of Shwachman–Diamond syndrome, including the failure of pancreatic progenitors to properly expand, nor was loss of p53 capable of rescuing the pancreatic defects associated with loss of other ribosome assembly factors, including *rpl3* and *pes*.[5]

We therefore sought to determine whether the failed expansion of pancreatic progenitors observed in *rpl23a* and *rpl6* mutant embryos could be rescued by loss of p53. Embryos generated by an *rpl23a*$^{hi2582/+}$;*ptf1a:eGFP*^{jh1};*ins:mCherry*^{jh2} incross were injected with a previously optimized dose of 1 ng of p53^{ATG} MO,[5] and the developing pancreas was assessed at 72 hpf (Fig. 4A, B). These studies demonstrated that p53 knockdown does not rescue abnormal pancreas development observed in *rpl23a*^{hi2582} mutant embryos. This appears to be true for both homozygote and heterozygote embryos, as there was no change in the fraction of phenotypic embryos among those injected with p53^{ATG} MO (67.7%) compared with mock-injected controls (69.2%) (Fig. 4B).

Next we incrossed our *rpl6*$^{hi3655b/+}$;*ptf1a:eGFP*^{jh1};*ins:mCherry*^{jh2} line and injected the embryos with 1 ng of p53^{ATG} MO. Similar to our findings regarding *rpl23a*, we observed no rescue of *ptf1a*-expressing pancreatic progenitor expansion in p53^{ATG} MO-injected embryos (Fig. 4C, D). There was no difference in the fraction of phenotypic embryos among those injected with p53^{ATG} MO (46.6%) compared with mock-injected controls (46.4%), suggesting that neither affected heterozygotes nor homozygotes are rescued by p53 knockdown. As in the case of prior observations made for *sbds*, *rpl3*, and *pes*, we conclude that defective expansion of *ptf1a*-expressing pancreatic progenitor cells observed in *rpl23a* and *rpl6* mutant embryos is a p53-independent phenomenon.

Discussion

We have demonstrated that multiple *rpl* genes display common temporal and spatial patterns of expression, characterized by highest level expression in developing endoderm- and endoderm-derived tissues, including the

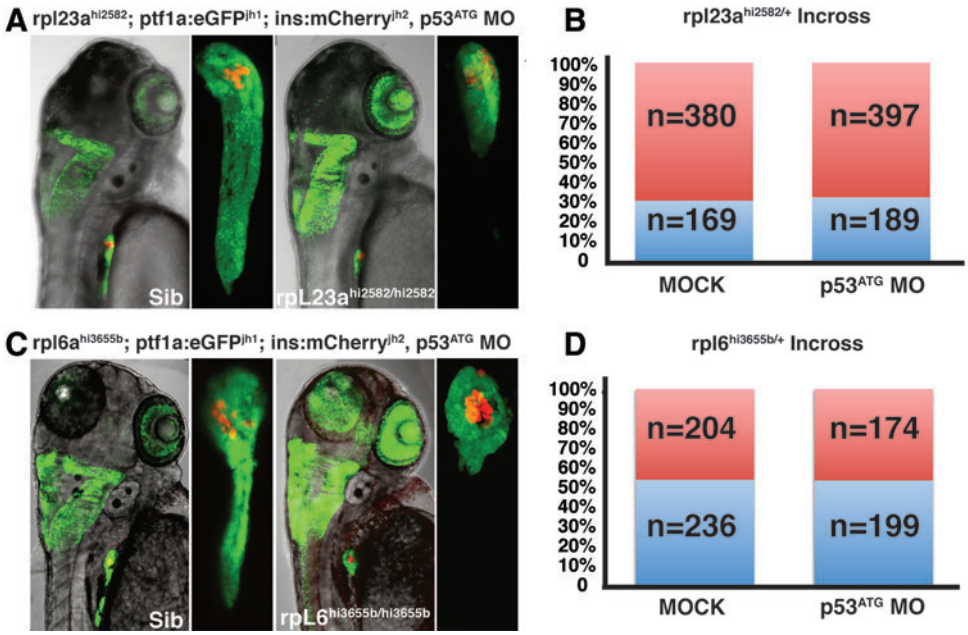

FIG. 4. Morpholino-mediated knockdown of p53 does fail to rescue defective expansion of *ptf1a*-expressing pancreas progenitor cells in *rpl* mutant embryos. **(A)** Injection of embryos produced by *rpl23a*$^{hi2582/+}$;*ptf1a:eGFP*^{jh1};*ins:mCherry*^{jh2} incross with 1 ng p53^{ATG} MO does not rescue hypoplastic pancreatic phenotype. **(B)** Incidence of abnormal pancreas development among embryos produced by *rpl23a*$^{hi2582/+}$;*ptf1a:eGFP*^{jh1};*ins:mCherry*^{jh2} incross injected with either p53^{ATG} MO or mock control (phenotypic, *red*; wild type, *blue*). **(C)** Injection of embryos produced by *rpl6*$^{hi3655b/+}$;*ptf1a:eGFP*^{jh1};*ins:mCherry*^{jh2} incross with 1 ng p53^{ATG} MO does not rescue hypoplastic pancreatic phenotype. **(D)** Incidence of abnormal pancreas development among embryos produced by *rpl6*$^{hi3655b/+}$;*ptf1a:eGFP*^{jh1};*ins:mCherry*^{jh2} incross injected with either p53^{ATG} MO or mock control (phenotypic, *red*; wild type, *blue*). Color images available online at www.liebertpub.com/zeb

developing pancreas. The observed high-level expression of *rpl* genes in undifferentiated *ptf1a*-expressing pancreatic progenitor cells suggests that these genes may play important roles in early pancreatic morphogenesis well before their role in supporting high levels of protein translation within differentiated acinar cells. Support for this hypothesis came from our previous work demonstrating a requirement for *rpl3* in the proliferative expansion of *ptf1a*-expressing pancreas progenitor cells.[5] To extend this work and determine whether defective pancreatic progenitor expansion represented a common consequence of *rpl* loss, we examined pancreas development in two additional mutant lines, $rpl23a^{hi2582}$ and $rpl6^{hi3655b}$. Our results demonstrate that at 72 hpf, when normal pancreas morphogenesis is nearly complete, $rpl23a^{hi2582/hi2582}$ and $rpl6^{hi3655b/hi3655b}$ homozygous embryos exhibit significant defects in *ptf1a*-expressing pancreatic progenitor expansion, similar to that previously reported for *rpl3*. These defects result in a hypoplastic pancreas, which in homozygote embryos shows no recovery over the next 24 h of development. Further, loss of even one copy of *rpl23a* or *rpl6* adversely affects the ability of pancreatic progenitors to undergo normal expansion. However, unlike homozygous embryos, heterozygotes are able to recover and complete their pancreatic developmental program, displaying a compensatory increase in pancreatic volume over the next 24 h of development. For both $rpl23a^{hi2582/hi2582}$ and $rpl6^{hi3655b/hi3655b}$ homozygous embryos, we observed that the hypoplastic pancreas underwent normal differentiation, as evidenced by activation of trypsin expression. Finally, we found that concomitant p53 knockdown fails to rescue defective pancreatic progenitor expansion in $rpl23a^{hi2582}$ or $rpl6^{hi3655b}$ homozygous or heterozygous embryos.

Currently, it is understood that disruption of ribosome biogenesis causes nucleolar stress that results in a characteristic p53-mediated cellular response. Evidence for this conclusion comes from biochemical studies demonstrating a physical interaction between specific RPs and the p53-inhibiting ubiquitin ligase mdm2, which results in p53 accumulation (reviewed[19]). Additionally, animal models of human disease with causal mutations in ribosome biogenesis genes, such as Diamond–Blackfan anemia, Treacher–Collins syndrome, and 5q− syndrome, have demonstrated induction of p53 and rescue upon concomitant inactivation of p53.[12–18] However, in a zebrafish model of another ribosome biogenesis disorder, Shwachman–Diamond syndrome, concomitant loss of p53 fails to rescue multiple developmental phenotypes associated with knockdown of the *sbds* gene. With regard to the pancreas, loss of either *sbds* or two other ribosome assembly genes (*rpl3* and *pes*) results in a p53-independent failure of *ptf1a*-expressing pancreatic progenitor expansion,[5] similar to that observed for *rpl23a* and *rpl6* in the current study. Thus, for each of the RPs and ribosome biogenesis genes evaluated to date, loss-of-function phenotypes converge upon a p53-independent mechanism of failed pancreatic progenitor expansion.

Together, these results reveal a requirement for an entire suite of *rpl* genes in early pancreas development, even while multiple other tissues are able to develop normally in the setting of altered *rpl* gene function. Together with prior reports of altered liver and gut development in *rpl* mutants (web.mit.edu/hopkins), our results suggest that developing endodermal tissues express uniquely high levels of *rpl* genes and are disproportionally sensitive to disruption of *rpl* gene function. Given the common view that genes related to ribosome biogenesis are expressed in excess within cells,[20] our finding that endoderm-derived tissues display uniquely high levels of *rpl* expression suggests the need for a more detailed understanding of *rpl* gene regulation. Beyond high-level expression, the basis for the heightened sensitivity of endoderm-derived tissues to *rpl* gene disruption remains uncertain, especially based on the ubiquitous requirement for ribosomes in all cell types. A component of this heightened sensitivity may be contributed to by developmental timing, with early developing ectoderm- and mesoderm-derived tissues potentially protected from zygotic *rpl* gene mutations by maternal *rpl* transcripts and/or protein, while the relatively later development of endoderm-derived tissues may be entirely dependent on zygotic expression. Alternatively, high levels of proliferation among pancreatic, liver, and gut progenitors may render these tissues highly sensitive to *rpl* disruption. Finally, each of these affected tissues ultimately generate large numbers of adult cells characterized by especially high-level protein synthesis and secretion, and the associated requirement for well-developed rough endoplasmic reticulum in these adult cell types may be presaged by a similar demand for high-level *rpl* expression in their embryonic progenitors.

It remains unclear whether or not the sensitivity of pancreatic, hepatic, and gut progenitor cells to *rpl* mutations reflects ribosomal versus nonribosomal functions of Rpl proteins. On the one hand, we have shown that a similar defect in the proliferative expansion of pancreatic progenitor cells induced by knockdown of zebrafish *sbds* is indeed associated with altered whole-embryo polysome profiles. However, this association has not been demonstrated to be causative, and RPs have recently been implicated in a wide variety of cellular functions, including DNA repair, transcriptional termination, cell cycle control, and leukocyte infiltration.[21–25] Thus, it appears likely that the defects in pancreas development observed in *rpl23a* and *rpl6* mutants reflect both ribosomal and extra-ribosomal functions of the *rpl23a* and *rpl6* gene products. Regardless of the mechanism involved, the current data demonstrate that *ptf1a*-expressing pancreatic progenitor cells are characterized by both high-level *rpl* expression and heightened sensitivity to *rpl* mutation. These findings may have relevance regarding the role of pancreatic progenitor cells not only in pancreas development, but also in regeneration and cancer.

Acknowledgments

The authors wish to thank Danielle Blake, Mary Chico, and Seneca Bessling for outstanding technical and administrative support. This work was supported by NIH grants R01 DK61215 (to S.D.L.) and T32 GM08752 to the Graduate Training Program in Cellular and Molecular Medicine.

Author Disclosure Statement

No competing financial interests exist.

References

1. Deisenroth C, Zhang Y. Ribosome biogenesis surveillance: probing the ribosomal protein-Mdm2-p53 pathway. Oncogene 2010;29:4253–4260.

2. Warner JR. The economics of ribosome biosynthesis in yeast. Trends Biochem Sci 1999;24:437–440.
3. Uechi T, Nakajima Y, Nakao A, Torihara H, Chakraborty A, Inoue K, *et al.* Ribosomal protein gene knockdown causes developmental defects in zebrafish. PLoS One 2006;1:e37.
4. Amsterdam A, Nissen RM, Sun Z, Swindell EC, Farrington S, Hopkins N. Identification of 315 genes essential for early zebrafish development. Proc Natl Acad Sci U S A 2004; 101:12792–12797.
5. Provost E, Wehner KA, Zhong X, Ashar F, Nguyen E, Green RA, *et al.* Ribosomal biogenesis genes play an essential and p53-independent role in pancreas development. Development 2012;139:3232–3241.
6. Narla A, Ebert BL. Ribosomopathies: human disorders of ribosome dysfunction. Blood 2010;115:3196–3205.
7. Godinho L, Williams PR, Claassen Y, Provost E, Leach SD, Kamermans M, *et al.* Nonapical symmetric divisions underlie horizontal cell layer formation in the developing retina *in vivo*. Neuron 2007;56:597–603.
8. Pisharath H, Rhee JM, Swanson MA, Leach SD, Parsons MJ. Targeted ablation of beta cells in the embryonic zebrafish pancreas using *E. coli* nitroreductase. Mech Dev 2007;124: 218–229.
9. Lin CH, Stoeck J, Ravanpay AC, Guillemot F, Tapscott SJ, Olson JM. Regulation of neuroD2 expression in mouse brain. Dev Biol 2004;265:234–245.
10. Biemar F, Argenton F, Schmidtke R, Epperlein S, Peers B, Driever W. Pancreas development in zebrafish: early dispersed appearance of endocrine hormone expressing cells and their convergence to form the definitive islet. Dev Biol 2001;230:189–203.
11. Falvey AK, Staehelin T. Structure and function of mammalian ribosomes. I. Isolation and characterization of active liver ribosomal subunits. J Mol Biol 1970;53:1–19.
12. Barlow JL, Drynan LF, Hewett DR, Holmes LR, Lorenzo-Abalde S, Lane AL, *et al.* A p53-dependent mechanism underlies macrocytic anemia in a mouse model of human 5q− syndrome. Nat Med 2010;16:59–66.
13. Jones NC, Lynn ML, Gaudenz K, Sakai D, Aoto K, Rey JP, *et al.* Prevention of the neurocristopathy Treacher Collins syndrome through inhibition of p53 function. Nat Med 2008;14:125–133.
14. Dixon J, Jones NC, Sandell LL, Jayasinghe SM, Crane J, Rey JP, *et al.* Tcof1/Treacle is required for neural crest cell formation and proliferation deficiencies that cause craniofacial abnormalities. Proc Natl Acad Sci U S A 2006;103:13403–13408.
15. Weiner AM, Scampoli NL, Calcaterra NB. Fishing the molecular bases of Treacher Collins syndrome. PLoS One 2012;7:e29574.
16. Danilova N, Sakamoto KM, Lin S. Ribosomal protein S19 deficiency in zebrafish leads to developmental abnormalities and defective erythropoiesis through activation of p53 protein family. Blood 2008;112:5228–5237.
17. Uechi T, Nakajima Y, Chakraborty A, Torihara H, Higa S, Kenmochi N. Deficiency of ribosomal protein S19 during early embryogenesis leads to reduction of erythrocytes in a zebrafish model of Diamond-Blackfan anemia. Hum Mol Genet 2008;17:3204–3211.
18. McGowan KA, Li JZ, Park CY, Beaudry V, Tabor HK, Sabnis AJ, *et al.* Ribosomal mutations cause p53-mediated dark skin and pleiotropic effects. Nat Genet 2008;40:963–970.
19. Chakraborty A, Uechi T, Kenmochi N. Guarding the 'translation apparatus': defective ribosome biogenesis and the p53 signaling pathway. Wiley Interdiscip Rev RNA 2011; 2:507–522.
20. Lam YW, Lamond AI, Mann M, Andersen JS. Analysis of nucleolar protein dynamics reveals the nuclear degradation of ribosomal proteins. Curr Biol 2007;17:749–760.
21. Kim TS, Kim HD, Kim J. PKCdelta-dependent functional switch of rpS3 between translation and DNA repair. Biochim Biophys Acta 2009;1793:395–405.
22. Torres M, Condon C, Balada JM, Squires C, Squires CL. Ribosomal protein S4 is a transcription factor with properties remarkably similar to NusA, a protein involved in both non-ribosomal and ribosomal RNA antitermination. EMBO J 2001;20:3811–3820.
23. Nishiura H, Zhao R, Yamamoto T. The role of the ribosomal protein S19 C-terminus in altering the chemotaxis of leucocytes by causing functional differences in the C5a receptor response. J Biochem 2011;150:271–277.
24. Warner JR, McIntosh KB. How common are extraribosomal functions of ribosomal proteins? Mol Cell 2009;34:3–11.
25. Bhavsar RB, Makley LN, Tsonis PA. The other lives of ribosomal proteins. Hum Genomics 2010;4:327–344.

Address correspondence to:
Steven D. Leach
McKusick-Nathans Institute of Genetic Medicine
Johns Hopkins University
733 North Broadway/BRB471
Baltimore, MD 21205

E-mail: stleach@jhmi.edu